https://doi.org/10.1016/j.apm.2019.07.040

Classification and Analysis of Constraint Singularities for Parallel Mechanisms Using Differential Manifolds

Shuofei Yang, Yangmin Li*

The Hong Kong Polytechnic University, Department of Industrial and Systems Engineering,
Kowloon 999077, Hong Kong, China

Abstract: This paper presents investigations into classification and analysis of constraint singularities for parallel mechanisms. Parallel mechanisms (also called parallel manipulators or parallel robots) have wide applications in industry. The singularities tremendously affect their applications. Existing research works show that constraint singularity causes a mechanism to have instantaneous DoFs or bifurcated finite motions. However, the intrinsic differences among the conditions under which the specific constraint singularities happen have not been discussed. This paper is focused on these topics by using differential manifolds as mathematical tool. Firstly, the general mathematical models of parallel mechanisms are formulated by respectively describing their finite motions and instantaneous motions in forms of differential manifolds and their tangent spaces. Then, parallel mechanisms having bifurcated finite motions and instantaneous DoFs are modelled accordingly, and the constraint singularities are thus classified into two kinds by considering their influences on motions of mechanisms in both finite and instantaneous motion levels. Finally, two examples are given to further illustrate the theoretical analysis. This paper lays foundations for mathematical modelling and applications of parallel mechanisms with constraint singularities.

Keywords: Parallel mechanism; Constraint singularity; Differential manifold; Instantaneous DoFs; Bifurcated motions

1. Introduction

Parallel mechanism [1,2] is also known as parallel manipulator [3-5] or parallel robot [6,7]. It is composed by several serial mechanisms that share the same moving platform, and these serial mechanisms are called its limbs [8]. The research on parallel mechanisms is a hot topic in the area of mechanisms and robotics. Many parallel mechanisms having different types of degree-of-freedoms (DoFs) have been invented. Due to their outstanding kinematic and dynamic performances, parallel mechanisms are widely used in machining and manufacturing industries.

In the research of mechanisms, singularity is one of the most important issues. As discussed by Müller and Zlatanov [9], singularity is the phenomenon occurring at some specific poses of a mechanism and leads to that the mechanism will gain or lose its DoFs, and the singularities of any mechanisms are classified into six types: redundant input, redundant output, redundant passive motion and impossible output, impossible input, and increased instantaneous mobility. For parallel mechanisms, singularities contain actuation singularity and constraint singularity. Actuation singularity is defined as the phenomenon when velocities of the actuation joints in a parallel mechanism are linearly dependent. It will cause that the rank of the twist Jacobian matrix degenerates, and that the mechanism loses one or more DoFs. Actuation singularity happens in any parallel mechanisms including the six-DoF ones. The discussions on actuation singularity can be traced back to the early works on Jacobian modelling of parallel mechanisms that were carried out by Hunt [10]. As the counterpart of actuation singularity, constraint singularity is discovered in the phenomenon when constraint forces provided by different limbs in a parallel mechanism are linearly dependent [9]. The correlation among the constraint wrenches results in that the limbs' constraints imposing on the moving platform will no longer enough to restrict the mechanism's motions, so that the mechanism will gain one or more DoFs at its constraint-singular pose. Unlike actuation singularity, constraint singularity only occurs in lower-mobility parallel mechanisms with less than six DoFs. In recent years, constraint singularity attracts much attention from academia because of the wide application of lower-mobility parallel mechanisms in industry.

The concept of constraint singularity was introduced by Zlatanov, Bonev, and Gosselin [11,12], and intensity investigations on constraint singularity have been conducted since then. Through formulating singularity equation in explicit form, the constraint singularity analysis of a 3-UPU parallel mechanism was given by Gregorio [13]. In our paper, R, P, H, U, and S denote a rotational, a prismatic, a helical, a universal, and a spherical joint, respectively. Similar work was done by Lee and Hervé [14], and they found that the 3-UPU parallel mechanism generates 3-DoF finite translations and 2-DoF instantaneous rotations with respect to the constraint-singular pose. Through using the forward kinematic univariate, Srivatsan and Bandyopadhyay [15] proposed a new method for deriving the geometric condition of constraint singularities of parallel mechanisms, and they took a 3-RPS mechanism for example. Li and Hervé [16] synthesized some four-DoF parallel mechanisms with bifurcation of Schoenflies motion. These mechanisms generate bifurcated motions moving from the constraint-singular pose. Chablat, Kong, and Zhang [17] found a parallel mechanism with five bifurcated operation mode, and carried out its singularity analysis. Gogu [18] studied the singularities of two-translational and one-rotational parallel mechanisms with bifurcated spatial motions. In the meantime, some methods were put forward to reveal the intrinsic properties and to explain physical meanings of singularities. Liu, Lou, and Li [19] provided a geometric study on the singularities of parallel mechanisms by using differential forms of the constraint functions that associate with the mechanisms. Singularity analysis is one of the most important issues in the field of parallel manipulators. By taking into account motion/force transmissibility, Liu, Wu, and, Wang [20] proposed several performance indices for singularity analysis that can be used to measure the closeness to

* Corresponding Author: yangmin.li@polyu.edu.hk

singularities. These indices are suitable for both actuation and constraint singularities.

The above analysis shows that many effectors have been carried out on the research of constraint singularity. However, it should be pointed out that there are some questions that are worthy of further investigations:

(1) Some constraint singularities (such as that of 3-UPU parallel mechanism) lead to instantaneous DoFs, while others (such as that of the parallel mechanism with bifurcated Schoenflies motion) lead to bifurcated finite motions. What are the differences between their constraint singularities in both finite and instantaneous motion levels?

(2) The singularities are classified into actuation singularity and constraint singularity by whether the instantaneous DoFs of the mechanism decreases or increases. Referring to this, how should the different kinds of constraint singularities be classified in finite and instantaneous motion levels?

These questions can be answered by studying the classification of constraint singularities. And the influences of different constraint singularities on both finite and instantaneous motions of parallel mechanisms can help to understand the motion characteristics of the mechanisms and to extend its applications.

As differential manifold theory together with screw theory has been successfully used in type synthesis [21,22], kinematic and dynamic [23,24] analysis of parallel mechanisms, we will use these mathematical tools for finite and instantaneous motion modelling and singularity analysis of parallel mechanisms in this paper.

The outline of the paper is listed as follows. The importance of singularity in the research and application of parallel mechanisms is addressed, and a brief review of the-state-of-art of constraint singularities is given in Section 1. In Section 2, through using differential manifolds and their tangent spaces, the general mathematical models of finite and instantaneous motions of parallel mechanisms are formulated in matrix form and in screw form, respectively. Considering the influences of constraint singularities on motions of mechanisms as well as the relationships between the twist and wrench spaces of mechanisms and their limbs, the constraint singularities are classified into two kinds in Section 3, and the mathematical nature of the classification is given in detail. In Section 4, two examples are given to verify the theoretical analysis. The conclusions are drawn in Section 5.

2. Mathematical modelling of parallel mechanisms' motions

Similar with the existing works [25,26], we use the sub-sets in the matrix representation of the Special Euclidean group SE(3) which acts on the six-dimensional real vector space ($\mathbb{R}^6$) to describe finite motions of parallel mechanisms. Meanwhile, the tangent spaces of these sub-sets are used to describe the mechanisms' instantaneous motions.

The motions of a parallel mechanism are determined by the motions of all the joints in it. The finite motions generated by one-DoF joints are described by one-parameter Lie groups, as listed in Table 1, where $\boldsymbol{s}$ and $\boldsymbol{r}$ with specific subscripts denote the unit direction vectors ($|\boldsymbol{s}_{\mathrm{R}}|=1$, $|\boldsymbol{s}_{\mathrm{P}}|=1$, $|\boldsymbol{s}_{\mathrm{H}}|=1$) and their perpendicular position vectors ($\boldsymbol{r}_{\mathrm{R}}^{\mathrm{T}}\boldsymbol{s}_{\mathrm{R}}=0$, $\boldsymbol{r}_{\mathrm{H}}^{\mathrm{T}}\boldsymbol{s}_{\mathrm{H}}=0$) of the corresponding joints, θ or t with specific subscripts are the rotational angles or translational distance of the corresponding joints from their initial poses, h is the pitch of the H joint; matrix $\boldsymbol{R}(\boldsymbol{s}_{\mathrm{R}},\boldsymbol{r}_{\mathrm{R}})$ denotes the rotation generated by the R joint with parameter θ_{R}, and the set $\{\boldsymbol{R}(\boldsymbol{s}_{\mathrm{R}},\boldsymbol{r}_{\mathrm{R}})\}$ (one-parameter matrix Lie group) denotes all the joint's rotations with parameter range as $\theta_{\mathrm{R}}\in[0,2\pi]$; $\boldsymbol{T}(\boldsymbol{s}_{\mathrm{P}})$ denotes the translation generated by the P joint with parameter t_{P}, and $\{\boldsymbol{T}(\boldsymbol{s}_{\mathrm{P}})\}$ denotes all its translations with $t_{\mathrm{P}}\in\mathbb{R}$; $\boldsymbol{H}(\boldsymbol{s}_{\mathrm{H}},\boldsymbol{r}_{\mathrm{H}},h)$ denotes the helical motion (combined by rotation and translation) generated by the H joint with parameter θ_{H}, and $\{\boldsymbol{H}(\boldsymbol{s}_{\mathrm{H}},\boldsymbol{r}_{\mathrm{H}},h)\}$ denotes all its motions with $\theta_{\mathrm{H}}\in\mathbb{R}$. In the expressions of the matrices, a vector followed by the cross product "$\times$" in the brackets "$[\ \ ]$" denotes the skew-symmetric matrix of the vector, such as $[\boldsymbol{s}_{\mathrm{R}}\times]$; $\boldsymbol{0}_{3\times3}$ is the 3×3 null matrix, and $\boldsymbol{E}_3$ is the three-order unit matrix.

Table 1 The finite motions generated by one-DoF joints.

Joint	Finite motions	Parameter
R	$\{\boldsymbol{R}(\boldsymbol{s}_{\mathrm{R}},\boldsymbol{r}_{\mathrm{R}})\}=\left\{\begin{bmatrix}\exp(\theta_{\mathrm{R}}[\boldsymbol{s}_{\mathrm{R}}\times]) & [(\boldsymbol{r}_{\mathrm{R}}-\exp(\theta_{\mathrm{R}}[\boldsymbol{s}_{\mathrm{R}}\times])\boldsymbol{r}_{\mathrm{R}})\times]\exp(\theta_{\mathrm{R}}[\boldsymbol{s}_{\mathrm{R}}\times]) \\ \boldsymbol{0}_{3\times3} & \exp(\theta_{\mathrm{R}}[\boldsymbol{s}_{\mathrm{R}}\times])\end{bmatrix}\right\}$	$\theta_{\mathrm{R}}\in[0,2\pi]$
P	$\{\boldsymbol{T}(\boldsymbol{s}_{\mathrm{P}})\}=\left\{\begin{bmatrix}\boldsymbol{E}_3 & t_{\mathrm{P}}\boldsymbol{s}_{\mathrm{P}} \\ \boldsymbol{0}_{3\times3} & \boldsymbol{E}_3\end{bmatrix}\right\}$	$t_{\mathrm{P}}\in\mathbb{R}$
H	$\{\boldsymbol{H}(\boldsymbol{s}_{\mathrm{H}},\boldsymbol{r}_{\mathrm{H}},h)\}=\left\{\begin{bmatrix}\exp(\theta_{\mathrm{H}}[\boldsymbol{s}_{\mathrm{H}}\times]) & [(\boldsymbol{r}_{\mathrm{H}}-\exp(\theta_{\mathrm{H}}[\boldsymbol{s}_{\mathrm{H}}\times])\boldsymbol{r}_{\mathrm{H}}+h\theta_{\mathrm{H}}\boldsymbol{s}_{\mathrm{H}})\times]\exp(\exp(\theta_{\mathrm{H}}[\boldsymbol{s}_{\mathrm{H}}\times])) \\ \boldsymbol{0}_{3\times3} & \exp(\theta_{\mathrm{H}}[\boldsymbol{s}_{\mathrm{H}}\times])\end{bmatrix}\right\}$	$\theta_{\mathrm{H}}\in\mathbb{R}$

Suppose that a parallel mechanism is composed by l limbs, and the No. i limb ($i = 1, 2, \cdots, l$) (the limbs are numbered arbitrarily) consists of n_i one-DoF joints, as shown in Fig. 1. Because each limb motion is composited by the motions of joints contained in it, and the mechanism motion is the intersection of all the limb motions, the finite motion of the parallel mechanism is modelled as

$$\boldsymbol{M}_{\mathrm{PM}} = \boldsymbol{M}_1 \bigcap \boldsymbol{M}_2 \cdots \bigcap \boldsymbol{M}_l \,, \tag{1}$$

while each limb motion is modelled as

$$\boldsymbol{M}_i = \boldsymbol{M}_{i,n_i} \bullet \cdots \bullet \boldsymbol{M}_{i,2} \bullet \boldsymbol{M}_{i,1} , \quad i = 1, 2, \cdots, l \,, \tag{2}$$

where $\boldsymbol{M}_{\mathrm{PM}}$, $\boldsymbol{M}_i$, and $\boldsymbol{M}_{i,k}$ denote the sets of finite motions of the parallel mechanism, its No. i limb, and the No. k joint ($k = 1, 2, \cdots, n_i$) (the joints in a limb are numbered from the one connected to the fixed base to the one connected to the moving platform in ascending order) in that limb; for each joint motion, $\boldsymbol{M}_{i,k}$ is in form of a one-parameter matrix Lie group in Table 1. The product "$\bullet$" of two matrix Lie groups results in the set that contains the multiplications of any two matrices, in which the first matrix is in the first Lie group and the second matrix is in the second Lie group.

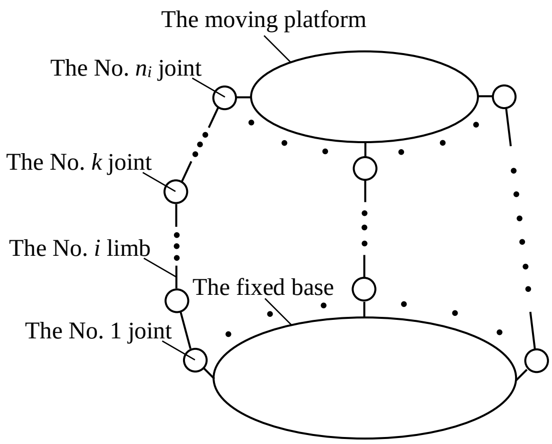

Fig. 1 Parallel mechanism composed by l limbs.

Since the direction vector, the position vector, and the motion parameter of each joint are measured at the parallel mechanism's initial pose, $\boldsymbol{M}_{\mathrm{PM}}$ describes all the finite motions that can be realized by the parallel mechanism from its initial pose. As each $\boldsymbol{M}_{i,k}$ is a Lie group, $\boldsymbol{M}_i$ is a Lie group or a general differential manifold of matrices. In this way, it is easy to know that $\boldsymbol{M}_{\mathrm{PM}}$ has the algebraic structure of Lie group, or general differential manifold, or the union of differential manifolds.

At any pose of the parallel mechanism, the instantaneous motions of the mechanism, each of its limbs and joints are described by the tangent spaces of $\boldsymbol{M}_{\mathrm{PM}}$, $\boldsymbol{M}_i$, and $\boldsymbol{M}_{i,k}$ at the pose, which means that

$$\boldsymbol{T}_{\mathrm{PM}} = \dot{\boldsymbol{M}}_{\mathrm{PM}} \Big|_{\substack{\text{paramters values of all the joints} \\ \text{in the mechanism at the pose}}} , \tag{3}$$

$$\boldsymbol{T}_i = \dot{\boldsymbol{M}}_i \Big|_{\substack{\text{paramters values of the } n_i \text{ joints} \\ \text{in the No. } i \text{ limb at the pose}}} , \tag{4}$$

$$\boldsymbol{T}_{i,k} = \dot{\boldsymbol{M}}_{i,k} \Big|_{\substack{\text{paramters value of the No. } k \text{ joint} \\ \text{in the No. } i \text{ limb at the pose}}} , \quad i = 1, 2, \cdots, l \,, \quad k = 1, 2, \cdots, n_i \,, \tag{5}$$

where $\boldsymbol{T}_{\mathrm{PM}}$, $\boldsymbol{T}_i$, and $\boldsymbol{T}_{i,k}$ are the twist spaces of the parallel mechanism, its No. i limb, and the No. k joint in the No. i limb at that pose of the mechanism. It should be noted that the twist spaces in matrix form can be directly rewritten into its isomorphic spaces in screw form [25].

3. Classification of constraint singularities for parallel mechanisms

Constraint singularity is a phenomenon occurring in a parallel mechanism when the wrench space spanned by the constraint wrenches of all limbs loses rank. In other words, the constraint wrenches provided by all limbs are not enough to constrain the mechanism motions. According to the reciprocal relationship between twist space and constraint wrench space, at the constraint singularity pose of a parallel mechanism, the intersection of the twist spaces of all limbs has more DoFs than its actual DoFs.

The existing works about constraint singularity focus on the degeneration of wrench space and the increment of twist space at the singularity pose, only the influences on instantaneous motions are taken into account. However, these works have not revealed the reason why singularity pose occurs and the influences that constraint singularity brings to the parallel mechanism on its finite motions. In this section, these topics will be investigated through discussing the classification of constraint singularities.

For a common pose at which constraint singularity does not occur, the tangent space of the mechanism manifold equals to the intersection of tangent spaces of the limb manifolds, which means that the mechanism's twist space equals to the interaction of all its limbs' twist spaces, as

$$\begin{aligned} \boldsymbol{T}_{\mathrm{PM}} &= \boldsymbol{T}_1 \cap \boldsymbol{T}_2 \cap \cdots \cap \boldsymbol{T}_l \\ &= \bigcap_{i=1,2,\cdots,l} \boldsymbol{T}_i \end{aligned} . \tag{6}$$

It also means that the mechanism's constraint wrench space is spanned by the constraint wrenches of all the limbs, as

$$\begin{aligned} \boldsymbol{W}_{\mathrm{PM}} &= \mathrm{span}\left\{\boldsymbol{W}_1 \cup \boldsymbol{W}_2 \cup \cdots \cup \boldsymbol{W}_l\right\} \\ &= \mathrm{span}\left\{\bigcup_{i=1,2,\cdots,l} \boldsymbol{W}_i\right\} \end{aligned} , \tag{7}$$

where $\boldsymbol{W}_{\mathrm{PM}}$ and $\boldsymbol{W}_i$ ($i = 1, 2, \cdots, l$) are the constraint wrench spaces of the parallel mechanism and its limbs at the pose. $\boldsymbol{W}_i$ of each limb is the reciprocal space (null space) of the corresponding $\boldsymbol{T}_i$, as

$$\boldsymbol{W}_i^{\perp} = \boldsymbol{T}_i, \quad i = 1, 2, \cdots, l . \tag{8}$$

Eqs. (6) and (7) are the regular way in which $\boldsymbol{T}_{\mathrm{PM}}$ and $\boldsymbol{W}_{\mathrm{PM}}$ are computed by the spaces of its limbs, and the obtained spaces are reciprocal to each other, i.e., $\boldsymbol{W}_{\mathrm{PM}} = \boldsymbol{T}_{\mathrm{PM}}^{\mathrm{T}}$. Both of these two equations are true at the common poses. However, for a constraint-singular pose, Eq. (6) will not hold; Eq. (7) will hold or not, and the constraint singularities for parallel mechanisms can thus be classified into two kinds accordingly.

3.1 Constraint singularity causing the bifurcation of finite motions

The first kind of constraint singularities causes the bifurcation of finite motions. When a parallel mechanism is at this kind of singular poses, Eq. (6) will not be true but Eq. (7) will still hold. The detailed explanation is given as follows.

If the singular pose is selected as the initial pose of the mechanism, its finite motions with bifurcation will be modelled as the union of two differential manifolds, as

$$\boldsymbol{M}_{\mathrm{PM}} = \boldsymbol{M}_A \cup \boldsymbol{M}_B , \tag{9}$$

which is continuous but not smooth at the initial pose. Hence, it is no longer a differential manifold and has no tangent space. In this situation, Eq. (3) does not hold. According to the relation between finite motions and instantaneous motions of a parallel mechanism, $\boldsymbol{T}_{\mathrm{PM}}$ is the union of the tangent spaces of the two differential manifolds contained in $\boldsymbol{M}_{\mathrm{PM}}$, as

$$\begin{aligned} \boldsymbol{T}_{\mathrm{PM}} &= \dot{\boldsymbol{M}}_A \Big|_{\substack{\text{all the joints paramters} \\ \text{are zero}}} \cup \dot{\boldsymbol{M}}_B \Big|_{\substack{\text{all the joints paramters} \\ \text{are zero}}} \\ &= \boldsymbol{T}_A \cup \boldsymbol{T}_B \end{aligned} . \tag{10}$$

At the bifurcation pose, $\boldsymbol{T}_A \cup \boldsymbol{T}_B$ contains all the common twists in all the limbs' twist spaces. Thus, $\bigcap_{i=1,2,\cdots,l} \boldsymbol{T}_i$ is computed as

$$\bigcap_{i=1,2,\cdots,l} \boldsymbol{T}_i = \mathrm{span}\left\{\boldsymbol{T}_A \cup \boldsymbol{T}_B\right\} . \tag{11}$$

It is easy to see that $\boldsymbol{T}_A \cup \boldsymbol{T}_B$ is not a linear space, it does not equal to $\mathrm{span}\left\{\boldsymbol{T}_A \cup \boldsymbol{T}_B\right\}$. Hence, comparing the above two equations, it can be obtained that Eq. (7) turns to be wrong.

When the first kind of constraint singularities occurs, as $\boldsymbol{T}_{\mathrm{PM}}$ is not a linear space and has no reciprocal space, $\boldsymbol{T}_{\mathrm{PM}}$ and $\boldsymbol{W}_{\mathrm{PM}}$ are no longer reciprocal to each other, i.e., $\boldsymbol{W}_{\mathrm{PM}} \neq \boldsymbol{T}_{\mathrm{PM}}^{\mathrm{T}}$. However, $\boldsymbol{W}_{\mathrm{PM}}$ still contains the wrenches that are reciprocal to all the twists in $\boldsymbol{T}_{\mathrm{PM}}$, so that it is computed as

$$\begin{aligned}\boldsymbol{W}_{\mathrm{PM}} &= \boldsymbol{T}_A^{\perp} \cap \boldsymbol{T}_B^{\perp} \\ &= \left(\operatorname{span}\left\{\boldsymbol{T}_A \cup \boldsymbol{T}_B\right\}\right)^{\perp}\end{aligned}. \tag{12}$$

Because constraint singularities only involve the relationship among motions and constraints of different limbs, they do not change the reciprocal relationship between twist and wrench spaces of each limb. Based upon Eq. (8), $\bigcup_{i=1,2,\cdots,l} \boldsymbol{W}_i$ is spanned to be

$$\begin{aligned}\operatorname{span}\left\{\bigcup_{i=1,2,\cdots,l} \boldsymbol{W}_i\right\} &= \operatorname{span}\left\{\bigcup_{i=1,2,\cdots,l} \boldsymbol{T}_i^{\perp}\right\} \\ &= \left(\bigcap_{i=1,2,\cdots,l} \boldsymbol{T}_i\right)^{\perp}\end{aligned}, \tag{13}$$

According to Eq. (11), Eqs. (13) and (14) show that Eq. (8) still holds at the bifurcation pose.

3.2 Constraint singularity causing no influence to finite motions but instantaneous DoFs

The second kind of constraint singularities causes no influence to finite motions but causes limbs' instantaneous DoFs. At this kind of singular poses, the twists and wrenches of a parallel mechanism will change without changing its finite motion characteristics. Both Eqs. (6) and (7) will not hold. The detailed explanation is given as follows.

Select any pose as the initial pose of the mechanism, its finite motions will be modelled as a differential manifold $\boldsymbol{M}_{\mathrm{PM}}$ in the usual way by solving the intersection of all its limb motions as shown in Eq. (1). And $\boldsymbol{T}_{\mathrm{PM}}$ at the singular pose is obtained through computing the differentiation of $\boldsymbol{M}_{\mathrm{PM}}$ at that pose by following Eq. (3). It is obvious that $\boldsymbol{T}_{\mathrm{PM}}$ has the same dimension with $\boldsymbol{M}_{\mathrm{PM}}$, which is coincident with the number of mechanism's DoFs. However, because of the constraint singularity, the dimension of $\bigcap_{i=1,2,\cdots,l} \boldsymbol{T}_i$ increases. It means that $\bigcap_{i=1,2,\cdots,l} \boldsymbol{T}_i$ has more base twists than $\boldsymbol{T}_{\mathrm{PM}}$, as

$$\bigcap_{i=1,2,\cdots,l} \boldsymbol{T}_i = \operatorname{span}\left\{\boldsymbol{T}_{\mathrm{PM}} \cup \boldsymbol{T}'\right\}, \tag{14}$$

where $\boldsymbol{T}'$ is a twist space spanned by the additional base twists caused by the constraint singularity. Thus, Eq. (6) does not hold.

Unlike the first kind of constraint singularities, at the second kind of constraint-singular poses, $\boldsymbol{T}_{\mathrm{PM}}$ is a linear space as usual, and the reciprocal relationship between $\boldsymbol{T}_{\mathrm{PM}}$ and $\boldsymbol{W}_{\mathrm{PM}}$ holds. $\boldsymbol{W}_{\mathrm{PM}}$ is obtained as

$$\boldsymbol{W}_{\mathrm{PM}} = \boldsymbol{T}_{\mathrm{PM}}^{\mathrm{T}}. \tag{15}$$

Meanwhile, using Eqs. (13) and (14), $\operatorname{span}\left\{\bigcup_{i=1,2,\cdots,l} \boldsymbol{W}_i\right\}$ is computed as

$$\begin{aligned}\operatorname{span}\left\{\bigcup_{i=1,2,\cdots,l} \boldsymbol{W}_i\right\} &= \left(\bigcap_{i=1,2,\cdots,l} \boldsymbol{T}_i\right)^{\perp} \\ &= \left(\operatorname{span}\left\{\boldsymbol{T}_{\mathrm{PM}} \cup \boldsymbol{T}'\right\}\right)^{\perp}\end{aligned}, \tag{16}$$

whose dimension is bigger than that of $\boldsymbol{W}_{\mathrm{PM}}$, so that Eq. (7) turns to be wrong.

As a summary, the differences between the two kinds of constraint singularities for parallel mechanisms are listed in Table 2. It can be easily seen that the constraint singularity of 3-UPU parallel mechanism belongs to the first kind, while the singularity of parallel mechanism having bifurcated Schoenflies motion belongs to the second.

Table 2 Comparison between two kinds of constraint singularities.

Constraint singularity	Influences on finite motions	Influences on instantaneous motions	Influences on constraint forces	Relationship between twist and wrench spaces
The first kind	Bifurcation	$\boldsymbol{T}_{\mathrm{PM}} \neq \bigcap_{i=1,2,\cdots,l} \boldsymbol{T}_i$	$\boldsymbol{W}_{\mathrm{PM}} = \operatorname{span}\left\{\bigcup_{i=1,2,\cdots,l} \boldsymbol{W}_i\right\}$	$\boldsymbol{W}_{\mathrm{PM}} \neq \boldsymbol{T}_{\mathrm{PM}}^{\mathrm{T}}$
The second kind	None	$\boldsymbol{T}_{\mathrm{PM}} \neq \bigcap_{i=1,2,\cdots,l} \boldsymbol{T}_i$	$\boldsymbol{W}_{\mathrm{PM}} \neq \operatorname{span}\left\{\bigcup_{i=1,2,\cdots,l} \boldsymbol{W}_i\right\}$	$\boldsymbol{W}_{\mathrm{PM}} = \boldsymbol{T}_{\mathrm{PM}}^{\mathrm{T}}$
None	N/A	$\boldsymbol{T}_{\mathrm{PM}} = \bigcap_{i=1,2,\cdots,l} \boldsymbol{T}_i$	$\boldsymbol{W}_{\mathrm{PM}} = \operatorname{span}\left\{\bigcup_{i=1,2,\cdots,l} \boldsymbol{W}_i\right\}$	$\boldsymbol{W}_{\mathrm{PM}} = \boldsymbol{T}_{\mathrm{PM}}^{\mathrm{T}}$

4. Examples

In this Section, two parallel mechanisms are given as examples to show the correctness of the theoretical results derived in Section 3. The first mechanism in Example A has the first kind constraint singularity; the second mechanism in Example B has the second kind constraint singularity.

4.1 Example A

Figure 2 shows a four-DoF parallel mechanism, which has been reported in [16]. Its moving platform has bifurcated Schoenflies motion with three translational DoFs and one bifurcated rotational DoF. It has two pairs of opposite limbs. Each limb in one pair is denoted as $P_aP_bP_cR_aR_b$, and each limb in the other pair is denoted as $P_bP_aP_cR_bR_a$. Thus, the mechanism can be denoted as 2-$P_aP_bP_cR_aR_b$-2-$P_bP_aP_cR_bR_a$. The directions of P_a, P_b, P_c, R_a, and R_b joints are $\boldsymbol{s}_a$, $\boldsymbol{s}_b$, $\boldsymbol{s}_c$, $\boldsymbol{s}_a$, and $\boldsymbol{s}_b$, respectively. The different unit direction vectors are drawn in different color in Fig. 2. The relationships between them are $\boldsymbol{s}_b \times \boldsymbol{s}_a = \boldsymbol{s}_c$. Observing from the top of the mechanism, the four limbs are numbered in counter-clockwise order. The three P joints with different directions in three limbs and an R joint in the fourth limb can be selected as actuation joints.

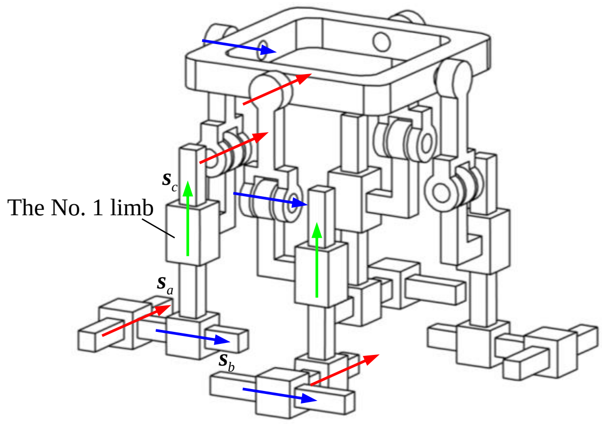

Fig. 2 A 2-$P_aP_bP_cR_aR_b$-2-$P_bP_aP_cR_bR_a$ parallel mechanism.

Select the symmetric pose of this parallel mechanism as its initial pose, as shown in Fig. 2. According to Eq. (2), the finite motion models of the four limbs are formulated as

$$\boldsymbol{M}_i = \{\boldsymbol{R}(\boldsymbol{s}_b, \boldsymbol{r}_{i,b})\} \cdot \{\boldsymbol{R}(\boldsymbol{s}_a, \boldsymbol{r}_{i,a})\} \cdot \{\boldsymbol{T}(\boldsymbol{s}_c)\} \cdot \{\boldsymbol{T}(\boldsymbol{s}_b)\} \cdot \{\boldsymbol{T}(\boldsymbol{s}_a)\}, \quad i = 1, 3, \tag{17}$$

and

$$\boldsymbol{M}_i = \{\boldsymbol{R}(\boldsymbol{s}_a, \boldsymbol{r}_{i,a})\} \cdot \{\boldsymbol{R}(\boldsymbol{s}_b, \boldsymbol{r}_{i,b})\} \cdot \{\boldsymbol{T}(\boldsymbol{s}_c)\} \cdot \{\boldsymbol{T}(\boldsymbol{s}_a)\} \cdot \{\boldsymbol{T}(\boldsymbol{s}_b)\}, \quad i = 2, 4, \tag{18}$$

where $\boldsymbol{r}_{i,a}$ ($\boldsymbol{r}_{i,a}^{\mathrm{T}} \boldsymbol{s}_a = 0$) and $\boldsymbol{r}_{i,b}$ ($\boldsymbol{r}_{i,b}^{\mathrm{T}} \boldsymbol{s}_b = 0$) are the position vectors of the R_a and R_b joints in the No. *i* limb, respectively.

Through algebraic derivations, the finite motions of the parallel mechanism are computed by solving the intersection of limb motions, which results in bifurcated motions as

$$\begin{aligned} \boldsymbol{M}_{\mathrm{PM}} &= \boldsymbol{M}_1 \cap \boldsymbol{M}_2 \cap \boldsymbol{M}_3 \cap \boldsymbol{M}_4 \\ &= \{\boldsymbol{R}(\boldsymbol{s}_a, \boldsymbol{r}_a)\} \cdot \{\boldsymbol{T}(\boldsymbol{s}_c)\} \cdot \{\boldsymbol{T}(\boldsymbol{s}_b)\} \cdot \{\boldsymbol{T}(\boldsymbol{s}_a)\} \cup \{\boldsymbol{R}(\boldsymbol{s}_b, \boldsymbol{r}_b)\} \cdot \{\boldsymbol{T}(\boldsymbol{s}_c)\} \cdot \{\boldsymbol{T}(\boldsymbol{s}_b)\} \cdot \{\boldsymbol{T}(\boldsymbol{s}_a)\}, \end{aligned} \tag{19}$$

where $\boldsymbol{r}_a$ and $\boldsymbol{r}_b$ respectively denote arbitrary position vectors. They can be any two three-dimensional vectors under conditions $\boldsymbol{r}_a^{\mathrm{T}} \boldsymbol{s}_a = 0$ and $\boldsymbol{r}_b^{\mathrm{T}} \boldsymbol{s}_b = 0$.

According to the analysis in Section 3.1, the twist and wrench spaces of the four limbs and the parallel mechanism are obtained as follows,

$$\boldsymbol{T}_i = \mathrm{span}\left\{ \begin{pmatrix} \boldsymbol{s}_a \\ \boldsymbol{r}_a \times \boldsymbol{s}_a \end{pmatrix}, \begin{pmatrix} \boldsymbol{s}_b \\ \boldsymbol{r}_b \times \boldsymbol{s}_b \end{pmatrix}, \begin{pmatrix} \boldsymbol{0} \\ \boldsymbol{s}_a \end{pmatrix}, \begin{pmatrix} \boldsymbol{0} \\ \boldsymbol{s}_b \end{pmatrix}, \begin{pmatrix} \boldsymbol{0} \\ \boldsymbol{s}_c \end{pmatrix} \right\}, \quad i = 1, 2, 3, 4, \tag{20}$$

$$\boldsymbol{W}_i = \mathrm{span}\left\{\begin{pmatrix}\boldsymbol{s}_c\\ \boldsymbol{0}\end{pmatrix}\right\}, \quad i=1,2,3,4, \tag{21}$$

and

$$\boldsymbol{T}_{\mathrm{PM}} = \mathrm{span}\left\{\begin{pmatrix}\boldsymbol{s}_a\\ \boldsymbol{r}_a\times\boldsymbol{s}_a\end{pmatrix},\begin{pmatrix}\boldsymbol{0}\\ \boldsymbol{s}_a\end{pmatrix},\begin{pmatrix}\boldsymbol{0}\\ \boldsymbol{s}_b\end{pmatrix},\begin{pmatrix}\boldsymbol{0}\\ \boldsymbol{s}_c\end{pmatrix}\right\}\cup\mathrm{span}\left\{\begin{pmatrix}\boldsymbol{s}_b\\ \boldsymbol{r}_b\times\boldsymbol{s}_b\end{pmatrix},\begin{pmatrix}\boldsymbol{0}\\ \boldsymbol{s}_a\end{pmatrix},\begin{pmatrix}\boldsymbol{0}\\ \boldsymbol{s}_b\end{pmatrix},\begin{pmatrix}\boldsymbol{0}\\ \boldsymbol{s}_c\end{pmatrix}\right\}, \tag{22}$$

$$\boldsymbol{W}_{\mathrm{PM}} = \mathrm{span}\left\{\begin{pmatrix}\boldsymbol{s}_c\\ \boldsymbol{0}\end{pmatrix}\right\}. \tag{23}$$

The relationships among these twist and wrench spaces can be obtained as

$$\boldsymbol{T}_{\mathrm{PM}} \neq \bigcap_{i=1,2,\cdots,l}\boldsymbol{T}_i = \mathrm{span}\left\{\begin{pmatrix}\boldsymbol{s}_a\\ \boldsymbol{r}_a\times\boldsymbol{s}_a\end{pmatrix},\begin{pmatrix}\boldsymbol{s}_b\\ \boldsymbol{r}_b\times\boldsymbol{s}_b\end{pmatrix},\begin{pmatrix}\boldsymbol{0}\\ \boldsymbol{s}_a\end{pmatrix},\begin{pmatrix}\boldsymbol{0}\\ \boldsymbol{s}_b\end{pmatrix},\begin{pmatrix}\boldsymbol{0}\\ \boldsymbol{s}_c\end{pmatrix}\right\}, \tag{24}$$

and

$$\boldsymbol{W}_{\mathrm{PM}} = \mathrm{span}\left\{\bigcup_{i=1,2,\cdots,l}\boldsymbol{W}_i\right\} = \mathrm{span}\left\{\begin{pmatrix}\boldsymbol{s}_c\\ \boldsymbol{0}\end{pmatrix}\right\}. \tag{25}$$

It is easy to see that the common wrench space of the parallel mechanism at other poses is

$$\boldsymbol{W}_{\mathrm{PM}} = \mathrm{span}\left\{\begin{pmatrix}\boldsymbol{s}_a\\ \boldsymbol{0}\end{pmatrix},\begin{pmatrix}\boldsymbol{s}_c\\ \boldsymbol{0}\end{pmatrix}\right\} \text{ or } \boldsymbol{W}_{\mathrm{PM}} = \mathrm{span}\left\{\begin{pmatrix}\boldsymbol{s}_b\\ \boldsymbol{0}\end{pmatrix},\begin{pmatrix}\boldsymbol{s}_c\\ \boldsymbol{0}\end{pmatrix}\right\}. \tag{26}$$

Comparing Eq. (26) with Eq. (24), it can be concluded that when the parallel mechanism is at the pose in Fig. 2, the dimension of its wrench space will decrease. This means that constraint singularity occurs at this pose. According to Eqs. (24) and (25), the union of the limbs' wrench spaces can still be spanned into the mechanism's wrench space, however, the intersection of the limbs' twist spaces does not equal to the mechanism's twist space. These conclusions are coincident with the theoretical results obtained in Section 3.1 and the first line in Table 2. Thus, the constraint singularity of the mechanism in Example A belongs to the first kind, which causes the bifurcation of the mechanism's finite motions as shown in Eq. (19).

4.2 Example B

Figure 3 shows a four-DoF parallel mechanism having Schoenflies motion. It is denoted as 2-$P_aP_bP_cR_dR_b$-2-$P_bP_aP_cR_dR_a$, which has been reported in [27]. Different with the mechanism in Fig. 2, its moving platform has three translational DoFs and one rotational DoF with fixed direction. It also has two pairs of opposite limbs. The directions of P_a, P_b, P_c, R_a, R_b, and R_d joints are $\boldsymbol{s}_a$, $\boldsymbol{s}_b$, $\boldsymbol{s}_c$, $\boldsymbol{s}_a$, $\boldsymbol{s}_b$, and $\boldsymbol{s}_d$, respectively, whose relationships are $\boldsymbol{s}_a\times\boldsymbol{s}_d=\boldsymbol{s}_c$ and $\boldsymbol{s}_b\times\boldsymbol{s}_d=\boldsymbol{s}_c$. The four limbs are numbered in counter-clockwise order, when they are observed from the top of the mechanism. Similar with the mechanism in Fig. 2, the three P joints with different directions in three limbs and an R joint in the fourth limb can be selected as actuation joints.

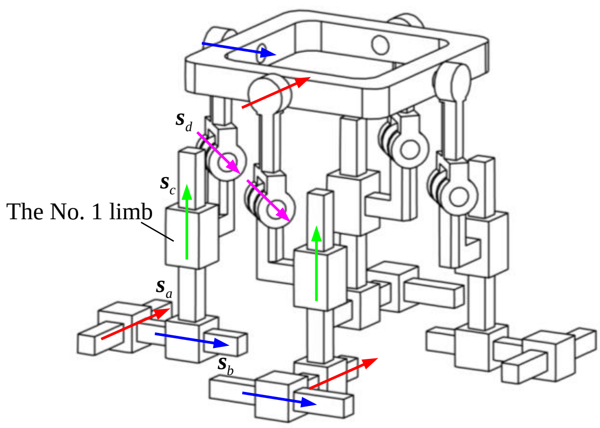

Fig. 3 A 2-$P_aP_bP_cR_dR_b$-2-$P_bP_aP_cR_dR_a$ parallel mechanism.

As shown in Fig. 3, the symmetric pose of the parallel mechanism is selected as its initial pose. The finite motion models of its four limbs are formulated by utilizing Eq. (2), as

$$\boldsymbol{M}_i = \left\{\boldsymbol{R}\left(\boldsymbol{s}_b, \boldsymbol{r}_{i,b}\right)\right\} \bullet \left\{\boldsymbol{R}\left(\boldsymbol{s}_d, \boldsymbol{r}_{i,d}\right)\right\} \bullet \left\{\boldsymbol{T}\left(\boldsymbol{s}_c\right)\right\} \bullet \left\{\boldsymbol{T}\left(\boldsymbol{s}_b\right)\right\} \bullet \left\{\boldsymbol{T}\left(\boldsymbol{s}_a\right)\right\}, \quad i = 1, 3, \tag{27}$$

and

$$\boldsymbol{M}_i = \left\{\boldsymbol{R}\left(\boldsymbol{s}_a, \boldsymbol{r}_{i,a}\right)\right\} \bullet \left\{\boldsymbol{R}\left(\boldsymbol{s}_d, \boldsymbol{r}_{i,d}\right)\right\} \bullet \left\{\boldsymbol{T}\left(\boldsymbol{s}_c\right)\right\} \bullet \left\{\boldsymbol{T}\left(\boldsymbol{s}_a\right)\right\} \bullet \left\{\boldsymbol{T}\left(\boldsymbol{s}_b\right)\right\}, \quad i = 2, 4, \tag{28}$$

where $\boldsymbol{r}_{i,a}$ ($\boldsymbol{r}_{i,a}^{\mathrm{T}} \boldsymbol{s}_a = 0$), $\boldsymbol{r}_{i,b}$ ($\boldsymbol{r}_{i,b}^{\mathrm{T}} \boldsymbol{s}_b = 0$), and $\boldsymbol{r}_{i,d}$ ($\boldsymbol{r}_{i,d}^{\mathrm{T}} \boldsymbol{s}_d = 0$) are the position vectors of the R_a, R_b, and R_d joints in the No. i limb, respectively.

Computing the intersection of limb motions by algebraic derivations, the finite motions of the parallel mechanism are obtained as

$$\begin{aligned} \boldsymbol{M}_{\mathrm{PM}} &= \boldsymbol{M}_1 \cap \boldsymbol{M}_2 \cap \boldsymbol{M}_3 \cap \boldsymbol{M}_4 \\ &= \left\{\boldsymbol{R}\left(\boldsymbol{s}_b, \boldsymbol{r}_b\right)\right\} \bullet \left\{\boldsymbol{R}\left(\boldsymbol{s}_d, \boldsymbol{r}_d\right)\right\} \bullet \left\{\boldsymbol{T}\left(\boldsymbol{s}_c\right)\right\} \bullet \left\{\boldsymbol{T}\left(\boldsymbol{s}_b\right)\right\} \bullet \left\{\boldsymbol{T}\left(\boldsymbol{s}_a\right)\right\} \cap \left\{\boldsymbol{R}\left(\boldsymbol{s}_a, \boldsymbol{r}_a\right)\right\} \bullet \left\{\boldsymbol{R}\left(\boldsymbol{s}_d, \boldsymbol{r}_d\right)\right\} \bullet \left\{\boldsymbol{T}\left(\boldsymbol{s}_c\right)\right\} \bullet \left\{\boldsymbol{T}\left(\boldsymbol{s}_b\right)\right\} \bullet \left\{\boldsymbol{T}\left(\boldsymbol{s}_a\right)\right\}, \\ &= \left\{\boldsymbol{R}\left(\boldsymbol{s}_d, \boldsymbol{r}_d\right)\right\} \bullet \left\{\boldsymbol{T}\left(\boldsymbol{s}_c\right)\right\} \bullet \left\{\boldsymbol{T}\left(\boldsymbol{s}_b\right)\right\} \bullet \left\{\boldsymbol{T}\left(\boldsymbol{s}_a\right)\right\} \end{aligned} \tag{29}$$

where $\boldsymbol{r}_a$, $\boldsymbol{r}_b$, and $\boldsymbol{r}_d$ are position vectors chosen arbitrarily, which can be any three three-dimensional vectors under conditions $\boldsymbol{r}_a^{\mathrm{T}} \boldsymbol{s}_a = 0$, $\boldsymbol{r}_b^{\mathrm{T}} \boldsymbol{s}_b = 0$, and $\boldsymbol{r}_d^{\mathrm{T}} \boldsymbol{s}_d = 0$.

Based upon the analysis in Section 3.2, through differentiating the finite motions models, the twist and wrench spaces of the four limbs and the parallel mechanism can be computed as the tangent spaces of the corresponding differential manifolds in Eqs. (27)-(29), as

$$\boldsymbol{T}_i = \operatorname{span}\left\{\begin{pmatrix} \boldsymbol{s}_b \\ \boldsymbol{r}_b \times \boldsymbol{s}_b \end{pmatrix}, \begin{pmatrix} \boldsymbol{s}_d \\ \boldsymbol{r}_d \times \boldsymbol{s}_d \end{pmatrix}, \begin{pmatrix} \boldsymbol{0} \\ \boldsymbol{s}_a \end{pmatrix}, \begin{pmatrix} \boldsymbol{0} \\ \boldsymbol{s}_b \end{pmatrix}, \begin{pmatrix} \boldsymbol{0} \\ \boldsymbol{s}_c \end{pmatrix}\right\}, \quad i = 1, 3, \tag{30}$$

$$\boldsymbol{T}_i = \operatorname{span}\left\{\begin{pmatrix} \boldsymbol{s}_a \\ \boldsymbol{r}_a \times \boldsymbol{s}_a \end{pmatrix}, \begin{pmatrix} \boldsymbol{s}_d \\ \boldsymbol{r}_d \times \boldsymbol{s}_d \end{pmatrix}, \begin{pmatrix} \boldsymbol{0} \\ \boldsymbol{s}_a \end{pmatrix}, \begin{pmatrix} \boldsymbol{0} \\ \boldsymbol{s}_b \end{pmatrix}, \begin{pmatrix} \boldsymbol{0} \\ \boldsymbol{s}_c \end{pmatrix}\right\}, \quad i = 2, 4, \tag{31}$$

$$\boldsymbol{W}_i = \operatorname{span}\left\{\begin{pmatrix} \boldsymbol{s}_c \\ \boldsymbol{0} \end{pmatrix}\right\}, \quad i = 1, 2, 3, 4, \tag{32}$$

and

$$\boldsymbol{T}_{\mathrm{PM}} = \operatorname{span}\left\{\begin{pmatrix} \boldsymbol{s}_d \\ \boldsymbol{r}_d \times \boldsymbol{s}_d \end{pmatrix}, \begin{pmatrix} \boldsymbol{0} \\ \boldsymbol{s}_a \end{pmatrix}, \begin{pmatrix} \boldsymbol{0} \\ \boldsymbol{s}_b \end{pmatrix}, \begin{pmatrix} \boldsymbol{0} \\ \boldsymbol{s}_c \end{pmatrix}\right\}, \tag{33}$$

$$\boldsymbol{W}_{\mathrm{PM}} = \operatorname{span}\left\{\begin{pmatrix} \boldsymbol{s}_c \\ \boldsymbol{0} \end{pmatrix}, \begin{pmatrix} \boldsymbol{s}_d \times \boldsymbol{s}_c \\ \boldsymbol{0} \end{pmatrix}\right\}. \tag{34}$$

Compare $\boldsymbol{T}_{\mathrm{PM}}$ and $\boldsymbol{W}_{\mathrm{PM}}$ with $\bigcap_{i=1,2,\cdots,l} \boldsymbol{T}_i$ and $\operatorname{span}\left\{\bigcup_{i=1,2,\cdots,l} \boldsymbol{W}_i\right\}$. The relationships among these twist and wrench spaces are

$$\boldsymbol{T}_{\mathrm{PM}} \neq \bigcap_{i=1,2,\cdots,l} \boldsymbol{T}_i = \operatorname{span}\left\{\begin{pmatrix} \boldsymbol{s}_a \\ \boldsymbol{r}_a \times \boldsymbol{s}_a \end{pmatrix}, \begin{pmatrix} \boldsymbol{s}_d \\ \boldsymbol{r}_d \times \boldsymbol{s}_d \end{pmatrix}, \begin{pmatrix} \boldsymbol{0} \\ \boldsymbol{s}_a \end{pmatrix}, \begin{pmatrix} \boldsymbol{0} \\ \boldsymbol{s}_b \end{pmatrix}, \begin{pmatrix} \boldsymbol{0} \\ \boldsymbol{s}_c \end{pmatrix}\right\}, \tag{35}$$

and

$$\boldsymbol{W}_{\mathrm{PM}} \neq \operatorname{span}\left\{\bigcup_{i=1,2,\cdots,l} \boldsymbol{W}_i\right\} = \operatorname{span}\left\{\begin{pmatrix} \boldsymbol{s}_c \\ \boldsymbol{0} \end{pmatrix}\right\}. \tag{36}$$

The twist and wrench spaces of the parallel mechanism at other poses are the same with those at this pose, while the intersection of its limbs' twist spaces at other poses is

$$\bigcap_{i=1,2,\cdots,l} \boldsymbol{T}_i = \text{span}\left\{ \begin{pmatrix} \boldsymbol{s}_d \\ \boldsymbol{r}_d \times \boldsymbol{s}_d \end{pmatrix}, \begin{pmatrix} \boldsymbol{0} \\ \boldsymbol{s}_a \end{pmatrix}, \begin{pmatrix} \boldsymbol{0} \\ \boldsymbol{s}_b \end{pmatrix}, \begin{pmatrix} \boldsymbol{0} \\ \boldsymbol{s}_c \end{pmatrix} \right\}. \tag{37}$$

It can be seen from Eqs. (36) and (37) that the dimension of the union of the limbs' wrench spaces decreases when the parallel mechanism is at the pose in Fig. 3. In other words, this pose is a constraint-singular pose of the mechanism. Even though Eqs. (35) and (36) show that the intersection of the limbs' twist spaces does not equal to the mechanism's twist space at the singular pose, and the union of the limbs' wrench spaces cannot be spanned into the mechanism's wrench space, the twist and wrench spaces of the mechanism remains unchanged at both the singular pose and other common poses. The above analyses are coincident with the theoretical results in Section 3.2 and the second line in Table 2. Hence, the constraint singularity of the mechanism in Example B belongs to the second kind, which brings no influence to the mechanism's finite motions but causes limbs' instantaneous DoFs as shown in Eqs. (29) and (35).

It should be pointed out that even though the two parallel mechanisms in Figs. 2 and 3 have the same number and types of joints, they are different mechanisms. Through the comparisons between Eqs. (19) and (29), between Eqs. (22) and (33), it can be concluded that their finite motions and instantaneous motions are different with each other. After comparing the structures of the mechanisms in the two Figures, we can see that the effect after turning the fourth joint in each limb to have the same direction changes the mechanism's motion from bifurcated Schoenflies motion to Schoenflies motion. This means that the rotation ability of the mechanism is changed from having two bifurcated rotational axes to having one fixed rotational axis. Therefore, the workspace of the mechanism in Fig. 2 with higher flexibility is larger than that of the mechanism in Fig. 3.

5. Conclusions

Through using differential manifolds and its tangent spaces as mathematical tool, in-depth investigations on classifications of constraint singularities for parallel mechanisms are presented. The following conclusions are drawn:

(1) The intrinsic differences between constraint singularities causing bifurcated motions and those causing instantaneous DoFs are revealed in both finite and instantaneous motion levels, leading to the classification of constraint singularities based upon relations between manifolds and tangent spaces of mechanisms and their limbs.

(2) Bifurcated motions and instantaneous DoFs of parallel mechanisms should be avoided in some situations. However, they can sometimes be utilized to realize specific tasks. The theoretical results in this paper give clear guidance for eliminating shakiness of some parallel mechanisms and designing parallel mechanisms with multi-operation modes.

Acknowledgment

This research work was supported in part by the research project of The Hong Kong Polytechnic University [Grant No. 1-45-37-ZE97]; in part by the General Research Fund (GRF) of Hong Kong Research Grants Council [Grant No. PolyU 152137/19E]; in part by the National Natural Science Foundation of China (NSFC) [Grant Nos. 51575544 and 51875391]; and in part by Natural Science Foundation of Tianjin City [Grant No. 16JCZDJC38000].

References

[1] X.X. Chai, Q.C. Li, W. Ye, Mobility analysis of overconstrained parallel mechanism using Grassmann–Cayley algebra, Applied Mathematical Modelling 51 (2017) 643-654.

[2] T. Sun, B.B. Lian, Y.M. Song, Stiffness analysis of a 2-DoF over-constrained RPM with an articulated traveling platform, Mechanism and Machine Theory 96 (2016) 165-178.

[3] Y. Lu, N.J. Ye, Y. Lu, Y.L. Wang, New kinematics Hessian matrixes of manipulators based on Skew-symmetric matrixes theory, Applied Mathematical Modelling 63 (2018) 55-67.

[4] A. Arian, B. Danaei, H. Abdi, S. Nahavandi, Kinematic and dynamic analysis of the Gantry-Tau, a 3-DoF translational parallel manipulator, Applied Mathematical Modelling 51 (2017) 217-231.

[5] B. Hu, J.J. Yu, Unified solving inverse dynamics of 6-DOF serial-parallel manipulators, Applied Mathematical Modelling 39 (16) (2015) 4715-4732.

[6] T. Sun, D. Liang, Y.M. Song, Singular-perturbation-based nonlinear hybrid control of redundant parallel robot, IEEE Transactions on Industrial Electronics 65 (4) (2018) 3326-3336.

[7] H.F. Ding, P. Huang, B. Zi, A. Kecskeméthy, Automatic synthesis of kinematic structures of mechanisms and robots especially for those with complex structures, Applied Mathematical Modelling 36 (12) (2012) 6122-6131.

[8] B.B. Lian, T. Sun, Y.M. Song, Parameter sensitivity analysis of a 5-DoF parallel manipulator, Robotics and Computer-Integrated Manufacturing 46 (2017) 1-14.

[9] A. Müller, D. Zlatanov, Singular Configurations of Mechanisms and Manipulators, Springer, Cham, 2019.

[10] K.H. Hunt, Kinematic Geometry of Mechanisms, Oxford University Press, Oxford, 1978.

[11] D. Zlatanov, I.A. Bonev, C.M. Gosselin, Constraint singularities of parallel mechanisms, In: Proceedings of the 2002 IEEE International Conference on Robotics and Automation, 2002, pp. 496-502.

[12] I.A. Bonev, D. Zlatanov, C.M. Gosselin, Singularity analysis of 3-DOF planar parallel mechanisms via screw theory, ASME Journal of Mechanical Design 125 (3) (2003) 573-581.

[13] R. D. Gregorio, Statics and singularity loci of the 3-UPU wrist, IEEE Transactions on Robotics 20 (4) (2004) 630-635.

[14] C.C. Lee, J.M. Hervé, Parallel mechanisms generating 3-DoF finite translation and (2 or 1)-DoF infinitesimal rotation, Mechanism and Machine Theory 51 (2012) 185-194.

[15] R.A. Srivatsan, S. Bandyopadhyay, Analysis of constraint equations and their singularities, In: J. Lenarčič, O. Khatib (eds), Advances in Robot Kinematics, Springer, Cham, 2014, pp. 429-436.
[16] Q.C. Li, J.M. Hervé, Parallel mechanisms with bifurcation of Schoenflies motion, IEEE Transactions on Robotics 25 (1) (2009) 158-164.
[17] D. Chablat, X.W. Kong, C.W. Zhang, Kinematics, workspace, and singularity analysis of a parallel robot with five operation modes, ASME Journal of Mechanisms and Robotics 10 (3) (2018) 035001-1-035001-12.
[18] G. Gogu, Maximally regular T2R1-type parallel manipulators with bifurcated spatial motion, ASME Journal of Mechanisms and Robotics 3 (1) (2011) 011010-1-011010-8.
[19] G.F. Liu, Y.J. Lou, Z.X. Li, Singularities of parallel manipulators: a geometric treatment, IEEE Transactions on Robotics and Automation, 19 (4) (2003) 579-594.
[20] X.J. Liu, C. Wu, J.S. Wang, A new approach for singularity analysis and closeness measurement to singularities of parallel manipulators, ASME Journal of Mechanisms and Robotics 4 (4) (2012) 041001-1-041001-10.
[21] T. Sun, X.M. Huo, Type synthesis of 1T2R parallel mechanisms with parasitic motions, Mechanism and Machine Theory 128 (2018) 412-428.
[22] Y. Qi, T. Sun, Y.M. Song, Type synthesis of parallel tracking mechanism with varied axes by modeling its finite motions algebraically, ASME Journal of Mechanisms and Robotics 9 (5) (2017) 054504-1-054504-6.
[23] D. Liang, Y.M. Song, T. Sun, Nonlinear dynamic modeling and performance analysis of a redundantly actuated parallel manipulator with multiple actuation modes based on FMD theory, Nonlinear Dynamics 89 (1) (2017) 391-428.
[24] T. Sun, Y.P. Zhai, Y.M. Song, J.T. Zhang, Kinematic calibration of a 3-DoF rotational parallel manipulator using laser tracker, Robotics and Computer-Integrated Manufacturing 41 (2016) 78-91.
[25] J. Meng, G.F. Liu, Z.X. Li, A geometric theory for analysis and synthesis of sub-6 DoF parallel manipulators, IEEE Transactions on Robotics 23 (4) (2007) 625-649.
[26] Y. Qi, T. Sun, Y.M. Song, Y. Jin, Topology synthesis of three-legged spherical parallel manipulators employing Lie group theory, Proceedings of the Institution of Mechanical Engineers, Part C: Journal of Mechanical Engineering Science 229 (10) (2015) 1873-1886.
[27] T.L. Yang, A.X. Liu, H.P. Shen, L.B. Hang, Y.F. Luo, Q. Jin, Topology Design of Robot Mechanisms, Springer, Singapore, 2018.